Journal of Pharmaceutical Innovation (2019) 14:50–56
https://doi.org/10.1007/s12247-018-9333-1

ORIGINAL ARTICLE

5-Fluorocytosine/5-Fluorouracil Drug-Drug Cocrystal: a New Development Route Based on Mechanochemical Synthesis

Cecilia C. P. da Silva[1,2] · Cristiane C. de Melo[1,3] · Matheus S. Souza[1] · Luan F. Diniz[1] · Renato L. Carneiro[2] · Javier Ellena[1]

Published online: 14 June 2018

Abstract

Purpose Mechanochemistry is addressed here for the green formation of a 1:1 pharmaceutical cocrystal involving the antifungal prodrug 5-Fluorocytosine (5-FC) and the antineoplastic drug 5-Fluorouracil (5-FU). Crystalline material of this drug-drug cocrystal (DDC) was previously obtained by slow evaporation from solution (SES) and was then structurally analyzed.

Method In this paper, neat grinding and solvent-drop grinding (SDG) were applied in an attempt to achieve a route for the supramolecular synthesis of this cocrystal, exhibiting suitable yield and amount for solid characterization, which were not achieved via the SES method.

Results SDG provided the solid drug-drug cocrystal form. The resulting material had its physical stability monitored for 2 years and was then evaluated by a range of analytical technologies: X-ray powder diffraction, differential scanning calorimetry, hot-stage microscopy, thermogravimetric, and spectroscopic analysis.

Conclusions The new cocrystal proved to be stable for 6 months and in environments with high relative humidity. In this sense, it is believed that the new DDC is a potential model system which could be used as a base for further developments in the field, for other molecules or in relation to the feasibility of using this cocrystal therapeutically.

Keywords Mechanochemistry · 5-Fluorocytosine · 5-Fluorouracil · Cocrystal · Physical stability · Solid-state characterization

Introduction

Pharmaceutical cocrystals—formed between an active pharmaceutical ingredient (API) and a cocrystal former (CF), solid under ambient conditions, not limited to two components, and having the compounds interacting by hydrogen bond or other non-covalent/non-ionic interaction—can be divided into two main groups: drug-coformer cocrystals (DCC), where at least one of the compounds is an API and the coformer(s) should belong to the generally recognized as safe (GRAS) list, and drug-drug cocrystals (DDC), composed at least by two different API molecules, being treated as a fixed-dose combination products. Literature concerning DCC is vast, but DDC are still rarely discussed. It is evident that the last few years have witnessed the emergence of this new field of crystal engineering and combination drugs delivery. As DDC represent unique solid forms of the parent APIs and cocrystallization do not alter the intrinsic activity of the APIs, there is an immense potential for physicochemical improvements resulting from the cocrystallization process. Therefore, there is a huge need to explore this class of compounds. This need arises by the fact that oral solid dosage forms of APIs are typically preferred, in a fashion that combining multiple drugs into a single dosage form may overcome problems associated with the traditional combination of drugs, improve clinical effectiveness, facilitate disease management, and minimize expenses related to pharmaceutical product manufacturing. Particularly, for APIs having similar molecular structures, the approach of solid solution may be applied, allowing the fine tuning of the desirable physicochemical properties for a particular combination of drugs, without the obligation of keeping fixed ratios between drugs.

✉ Javier Ellena
javiere@ifsc.usp.br

[1] Instituto de Física de São Carlos, Universidade de São Paulo, 369, São Carlos, Sao Paulo 13560-970, Brazil

[2] Departamento de Química, Universidade Federal de São Carlos, São Carlos, Sao Paulo 13083-887, Brazil

[3] Faculdade de Ciências Farmacêuticas, Universidade Federal de Alfenas, Alfenas, Minas Gerias 37130-000, Brazil

Moreover, there is also a strong need to explore methodologies to increase the likelihood of success in supramolecularly synthesizing DDCs [1–20].

Pharmaceutical Green Chemistry is an emerging issue concerning medicine production versus environmental impact. Considering that one of the most important aim of green chemistry is sustainability, minimizing the use of the planet's natural resources by discovering and developing efficient new synthetic pathways for drug production has become a challenge for pharmaceutical scientists. In this sense, solid-state grinding or mechanochemistry is an attractive green solution allowing reactions between two or more compounds with little or no waste generation. Over the past decades, an improvement in this synthesis method has been reported, known as solvent-drop grinding (SDG). In SDG, a controlled amount of solvent is added during the grinding process, favoring the formation kinetics of the new compound [21–34].

Herein, we report a SDG route for the supramolecular synthesis of a cocrystal containing two APIs (Scheme 1), namely 5-Fluorocytosine (4-amino-5-fluoro-1,2-dihydropyrimidin-2-one, 5-FC) and 5-Fluorouracil (5-fluoro-2,4-(1H,3H)-pyrimidinedione, 5-FU). 5-FU is an antineoplastic API used for the treatment of several cancers. 5-FC has become one of the most used prodrug for cancer treatment via gene-directed enzyme prodrug therapy (GDEPT) or suicide gene therapy [35–41]. This DDC was designed with the intention to offer the scientific community a model system that could be used as a base for further developments in the field, for applicability with other molecules or in relation to the feasibility of using this cocrystal therapeutically. The crystalline structure of this 1:1 cocrystal was previously reported by our group [42], as crystals obtained by slow evaporation of the solvent (SES). Nevertheless, SES has not yielded purity over the entire sample, thus not allowing the evaluation of the physical properties of this new cocrystal at the time. By SDG, however, the resulting amount of cocrystal achieved a satisfactory yield, allowing its thermal and spectroscopy evaluation, as well its physical stability assessment, which could be evaluated during 2 years. It is worth mentioning that the physical stability analysis was performed for the raw cocrystal and not for the cocrystal in a formulation.

Experimental Section

Synthesis by Neat Grinding 5-FC (150 mg, 1.2 mmol) and 5-FU (151 mg, 1.2 mmol) were co-milled using an oscillatory ball mill Mixer Mill MM400 RETSCH. The sample powder was placed in a 25-mL volume stainless steel milling jar containing two 7-mm diameter stainless steel balls. The system was milled at different frequencies/times at room temperature. At the end of each procedure, a sample was separated and analyzed by PXRD. The frequency/time that generated the best results was at 25 Hz for 90 min.

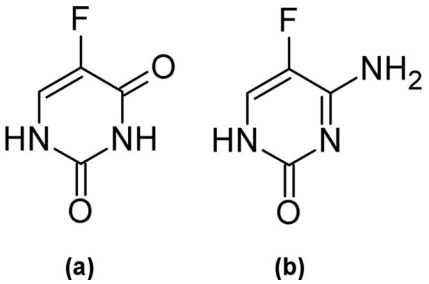

Scheme 1 Molecular structure of **a** 5–FU and **b** 5–FC

Synthesis by Solvent-Drop Milling 5-FC (150 mg, 1.2 mmol), 5-FU (151 mg, 1.2 mmol), and one drop of water were co-milled using an oscillatory ball mill Mixer Mill MM400 RETSCH. The sample powder was placed in a 25-mL volume stainless steel milling jar containing two 7-mm diameter stainless steel balls. The optimized final condition to obtain the multi-API cocrystal was achieved by milling the system at a frequency of 25 Hz, at room temperature, and 60 min.

Powder X-ray Diffraction The milled sample was analyzed using a Rigaku-Denki powder diffractometer. Experimental conditions: CuKα radiation, λ = 1.5418 Å; 50 kV; 100 mA; step scan with a step width of 0.01° at an interval of 10°–50° in 2θ; time per step 3 s.

Hot-Stage Polarized Optical Microscopy Microscopy was performed on a Leica DM2500P microscope connected to the Linkam T95-PE hot-stage equipment. Data were visualized with the Linksys 32 software for hot-stage control. One crystal was placed on a 13-mm glass coverslip, and placed on a 22-mm diameter pure silver heating block inside of the stage. The sample was heated at a ramp rate of 10 °C/min up to a final temperature of 300 °C, but discontinued on melting of all material.

Spectroscopic Analysis Raman spectra acquisition was performed in a B&W Tek i-Raman BWS 415-785H, with red laser (785 nm), spectral resolution of 2.5 cm^{-1}, and 120 s of acquisition time. For the Fourier transform infrared (FTIR) analysis, the sample was ground with dry KBr and further pressed. The KBr pellet was mounted in the FTIR sample holder and analyzed by a Shimadzu FTIR Prestige 21, using 128 scans over a range of 400–4000 cm^{-1} at 2 cm^{-1} of resolution. These experiments were conducted with the particular goal to state the stability of the cocrystal, especially under humidity conditions.

Thermal Analysis Thermogravimetric analysis was performed using a Shimadzu TGA-60 thermobalance. 3.500 ± 0.001 mg of the cocrystal was placed in an alumina pan and heated at 10 °C min^{-1} under a N_2 atmosphere (100 mL min^{-1}) from 30 to 320 °C. Differential scanning calorimetry (DSC) was

carried out by means of a Shimadzu DSC-60 calorimeter. The sample (approximately 3.00 ± 0.01 mg of the cocrystal; 2.60 ± 0.01 mg of the 5FC; 2.80 ± 0.01 mg of the 5FU) was heated from 30 to 310 °C with a heating rate of 10 °C min^{-1} in a crimped sealed aluminum pan. The purge gas was nitrogen under a flow of 100 mL min^{-1}. All the values reported here were extrapolated from the DSC curves using the Shimadzu TA-60 software (version 2.2).

Results and Discussions

The DDC of 5-FC with 5-FU, designed and synthesized by our group through water-based methods, have previously been characterized in terms of its crystal structure [42]. Briefly, in the cocrystal structure, there are homodimers of 5-FU and homodimers of 5-FC interacting to each other by single N–H···O hydrogen-bonds, constituting flat tapes of interspersed homounits. Although the formation of heterodimers among the APIs molecules was expected, currently this goal has not been achieved. Nevertheless, the interleaved flat tapes result in the formation of columns containing only 5-FU molecules and columns containing only 5-FC molecules (Fig. 1).

Neat Grinding Vs SDG The main goal of this work was to synthesize higher amounts of the 5-FC/5-FU DDC in order to evaluate its solid-state features. Thus, mechanochemical grinding was applied to the supramolecular synthesis of the cocrystal utilizing a ball milling equipment. Although this is a very useful technique, it is not a trivial task to achieve the best

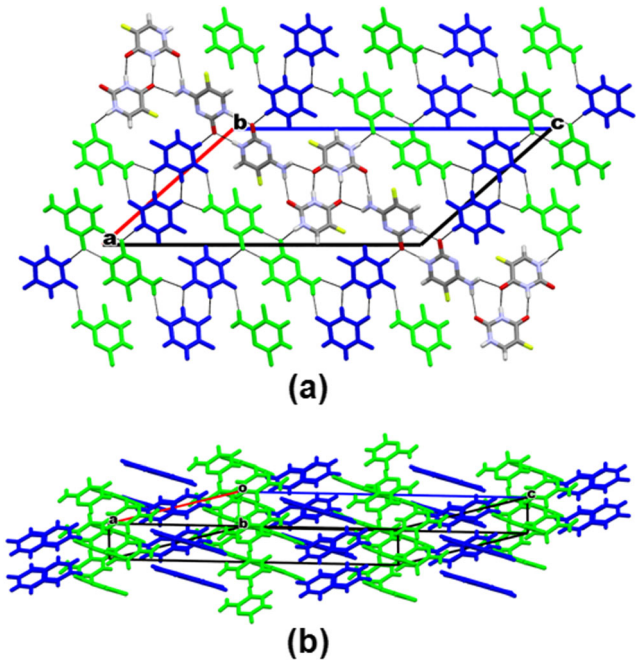

Fig. 1 Crystalline packing of the cocrystal evidencing **a** the intermolecular arrangement and **b** the resulting columns of each API

frequency and time where the compounds will encompass chemical reactions induced by the use of mechanical force. Therefore, neat grinding and SDG should both be tried. The final product yield utilizing both strategies is not significantly affected by the solubilities of the individual components, as is in the SES technique; however, the presence of a catalytic amount of solvent in SDG is known to enhance the molecular diffusion needed for molecular recognition which can be translated into improved efficiency of this strategy over neat grinding. Another advantage of SDG over neat grinding is that this strategy may yield significant amounts of an amorphous phase [32]. Several conditions were tested for achieving the cocrystal formation. As can be seen in Fig. 2, the resulting powder X-ray diffraction studies of the neat grinding (NG) samples generated two different patterns: one resembling a sum of both raw API's phases (Fig. 2, NG-1) and other one resembling the cocrystal phase (Fig. 2, NG-2), but containing amorphous phase. The addition of one drop of water, on the other hand, provided the catalytic condition necessary for yielding cocrystal formation, with no detectable amounts of amorphous by PXRD (absence of baseline shift, Fig. 2 - SDG) and DSC (absence of crystallization peaks, see Fig. 3a in the next section). SDG was repeated four times at the frequency and time mentioned in the experimental section, which was the best condition found. In these experiments, different amounts of the pure drugs were added. In all the experiments, satisfactory yield of the DDC was achieved.

Thermal Analysis The DSC curve of the cocrystal (Fig. 3a) is characterized by a sharp endothermic peak with a maximum at 282.19 °C and an associated enthalpy of $\Delta H = 44.87$ kJ/mol, which was assigned to the melting process of the cocrystal.

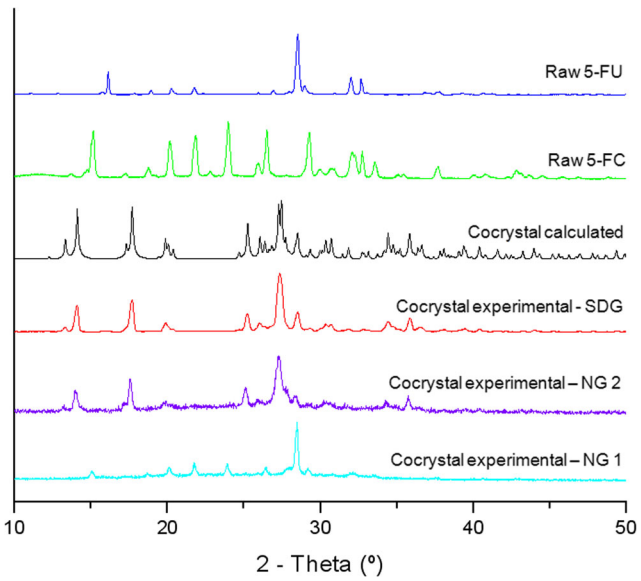

Fig. 2 Powder X-ray diffractograms of the cocrystal supramolecular synthesis by neat and solvent-drop grinding, compared with the raw materials

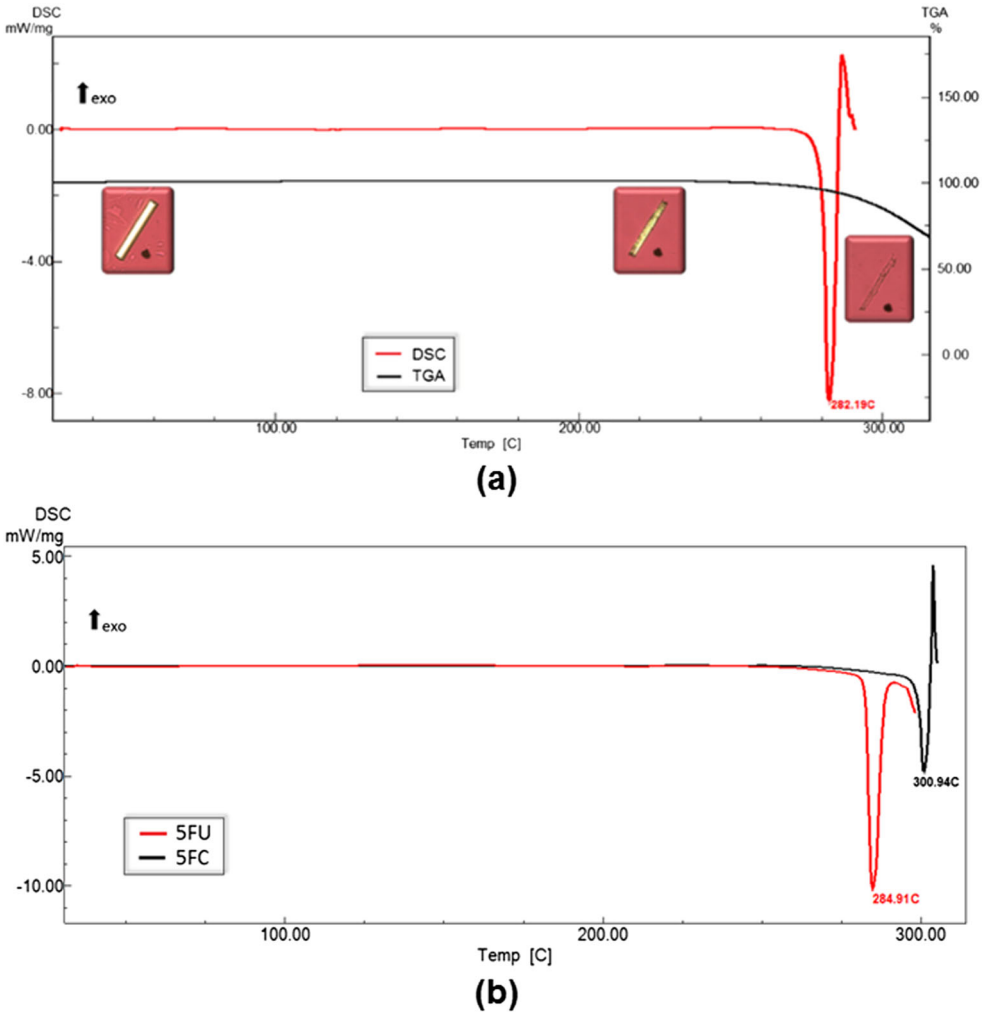

Fig. 3 DSC curves of the (a) cocrystal, superposed with the TGA, and evidencing the crystal behavior by hot-stage microscopy and (b) raw APIs

This event begins at 278.10 °C (onset temperature) and ends at 285.28 °C (endset temperature), being in agreement with the TGA curve, once there is no significant weight lost in the range of 30–285 °C. The DSC curve also exhibits an exothermic peak. As expected, this peak agrees with an abrupt weight lost in the TGA curve, indicating the temperature which cocrystal decomposition starts. In addition, as the DSC curve did not reveal any other peak that could be assigned to a phase transition, this result suggest the high purity of the material produced by SDG.

The thermal behavior of 5-FC and 5-FU was also analyzed (Fig. 3b), with the goal to establish a comparison between the cocrystal and the individual APIs. The DSC curve of pure 5-FU showed an endothermic melting peak with a maximum at 284.91 °C, which is almost the same temperature that melts the cocrystal. However, the heat of fusion for both compounds are different, which support the new obtained cocrystal. The pure 5-FU has a lower heat of fusion ($\Delta H = 26.35$ kJ/mol) than the cocrystal. On the other hand, pure 5-FC melts at a temperature several degrees higher than the cocrystal. The DSC curve of pure 5-FC is characterized by an endothermic melting peak with a maximum at 300.94 °C and an associated enthalpy of $\Delta H = 11.08$ kJ/mol.

Physical Stability The DDC of 5-FC with 5-FU had its physical stability evaluated, by PXRD, FTIR, and Raman spectroscopies, in terms of humidity effect over 1 and 2 weeks, and long-term storage over 6 months and 2 years. For the humidity study, the sample was submitted to 100% relative humidity using a desiccator with distilled water to obtain the desired humidity. The desiccator was sealed at room temperature (25 °C). The relative humidity and temperature therein were measured with a thermohygrometer properly calibrated. Prior to sample exposure, the desiccator opening was standardized, occurring once daily for 10 days, with the objective of simulating the sample data collection. As the humidity variation during this period did not exceed 5% and the temperature did not exceed 1 °C, the methodology was considered satisfactory. For the experiment, one portion of the DDC sample was stored in a glass vial at room temperature (~25 °C) without relative humidity control. Then, another portion was dried in an oven and placed in the desiccator. After 1 and 2 weeks,

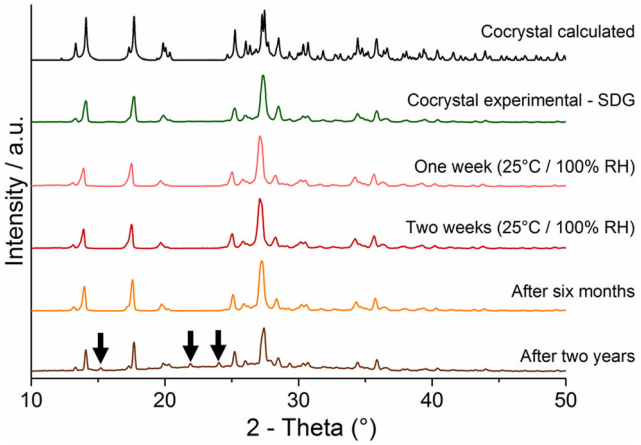

Fig. 4 PXRD diffractograms for the DDC after 1 and 2 weeks under 100% RH, and after 6 months and 2 years of storage. The black arrows in the 2-year diffractogram evidence phase transitions taking place in the sample

respectively, under the accelerated storage condition (high moisture content), the samples were removed from the desiccator and analyzed by PXRD. The PXRD patterns (Fig. 4) showed that the main characteristic peaks of the calculated diffractogram were in good agreement with the experimental one indicating that even in an environment with 100% relative humidity there was no significant change in the cocrystal crystallinity.

For the long-term storage study, the DDC sample was stored in a closed glass vial, at room temperature. PXRD was performed right before closing the vial, after 6 months, and after 2 years (Fig. 4). The same main characteristic peaks were observed in the PXRD experimental patterns of all samples. Exception can be applied for the 2-year diffractogram, which exhibits small peaks at 2-Theta values of 15°, 22°, and 24°, indicating the beginning of phase transitions taking place in the crystalline system. The rising of this crystalline phase could come from the crystallization of some remaining trace of undetected amorphous material (low probability, since it was not detectable by DSC and PXRD) or due the limited stability of the cocrystal (both APIs present higher melting points than the cocrystal, what is an indicative that the cocrystal is less stable than the parent APIs). Comparing these new peaks with the raw materials of 5-FC and 5-FU, it is possible to ascertain that they are related to the crystallization of raw 5-FC, which supports the assumption of a limited physical stability of the cocrystal.

FTIR and Raman spectra were taken right before closing the vial. Raman was repeated after 2 years. FTIR was used to evaluate stability after humidity experiments. The Raman and FTIR spectra of the 5-FC and 5-FU cocrystal are shown in Figs. 5 and 6, respectively. Both spectra show characteristic bands arising from the vibrational modes of 5-FC and 5-FU molecules. As can be seen in Scheme 1, 5-FC structurally differs from 5-FU by the presence of an amino group at position 6. The asymmetric stretching mode of the NH_2 group appears in the FTIR spectrum as a strong band at 3452 cm^{-1}, a frequency higher than that of the symmetrical one (3335 cm^{-1}). The bands at 1656, 1360, and 629 cm^{-1} in the FTIR can be assigned to the NH_2 scissoring, rocking, and wagging modes, respectively. The wagging mode is active in the Raman spectrum and appears at the same wavenumber, i.e., 629 cm^{-1}. These assignments were performed following the previous spectroscopic studies about 5-FC and 5-FU reported on the literature [42, 43]. In fact, these experiments were conducted to state the stability of the cocrystal under

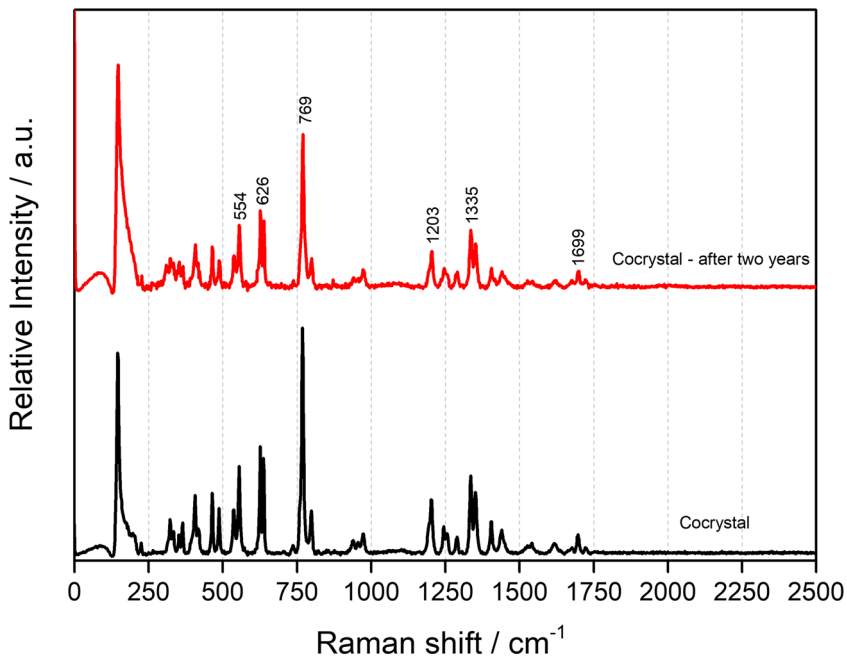

Fig. 5 Raman spectra of the DDC right after synthesis and after 2 years of storage

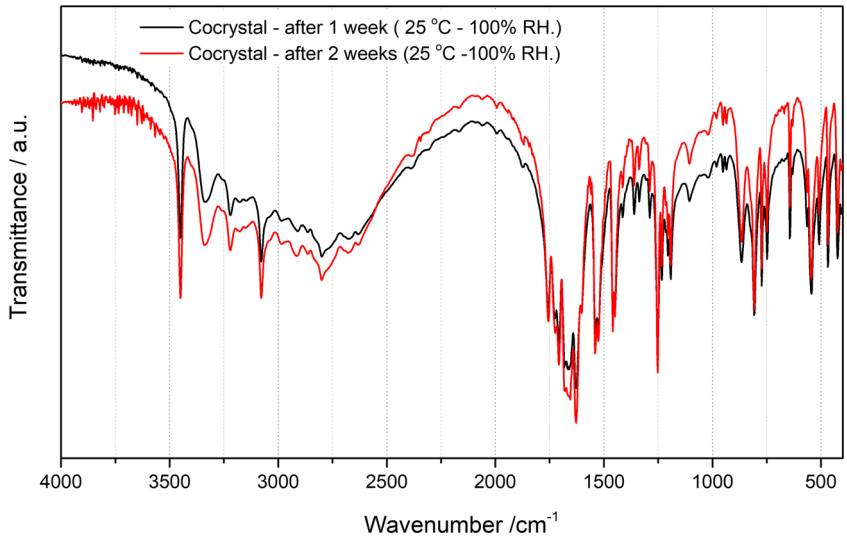

Fig. 6 FTIR spectra of the DDC after one (black) and after two (red) weeks under 100% RH

high humidity conditions. Likewise PXRD data, Raman spectra corroborate that there was no significant change in the cocrystal.

Conclusions

Mechanochemistry was successfully applied for the supramolecular synthesis of the drug-drug cocrystal involving the antineoplastic drug 5-Fluorouracil and its prodrug 5-Fluorocytosine. Neat and solvent-drop grinding were applied and compared. For the first method, none of the tested conditions led to cocrystal formation. On the other hand, when a catalytic amount of solvent was added before grinding, cocrystal formation was successfully achieved, demonstrating one more time that SDG may be an efficient route to cocrystal production with suitable yield. After synthesis was standardized, the cocrystal was evaluated in terms of thermal behavior and physical stability. It is noteworthy that the resulting cocrystal remains stable after 6 months of storage. Also, the cocrystal did not exhibited significant changes in an environment with 100% relative humidity. This physical stability is an essential feature when dealing with new pharmaceutical product candidates. However, for considering the feasibility of using this cocrystal therapeutically, further studies concerning its physical stability should be performed in the presence of an actual dosage form, where excipients and mechanical stress may be present. In addition, the success in mechanochemical supramolecular synthesis of this DDC opens the doors to the development of more flexible oral dosage forms.

Funding information The authors received financial support from CAPES (C.C.P.S. and M.S.S.), CNPq (C.C.M., J.E. grant #305190/2017-2), and FAPESP (L.F.D. grant #15/25694-0).

References

1. Aitipumala S, et al. Polymorphs, salts, and cocrystals: what's in a name? Cryst Growth Des. 2012;12(5):2147–52.
2. Surov AO, Voronin P, Manin AN, Manin NG, Kuzmina LG, Churakov AV, et al. Pharmaceutical cocrystals of diflusinal and diclofenac with theophylline. Mol Pharm. 2014;11(10):3707–15.
3. See US FDA GRAS List. http://www.fda.gov/food/ingredientspackaginglabeling/gras/default.htm.
4. See Regulatory Classification of Pharmaceutical Co-crystals Guidance for Industry. https://www.fda.gov/downloads/Drugs/Guidances/UCM281764.pdf.
5. Trask AV, Motherwell WDS, Jones W. Pharmaceutical cocrystallization: engineering a remedy for caffeine hydration. Cryst Growth Des. 2005;5(3):1013–21.
6. Vishweshwar P, McMahon JA, Bis JA, Zaworotko MJ. Pharmaceutical cocrystals. J Pharm Sci. 2006;95(3):499–516.
7. Berry DJ, Seaton CC, Clegg W, Harrington RW, Coles SJ, Horton PN, et al. Applying hot-stage microscopy to co-crystal screening: a study of nicotinamide with seven active pharmaceutical ingredients. Cryst Growth Des. 2008;8(5):1697–−1712.
8. Schultheiss N, Newman A. Pharmaceutical cocrystals and their physicochemical properties. Cryst Growth Des. 2009;9(6):2950–67.
9. Cheney ML, Shan N, Healey ER, Hanna M, Wojtas L, Zaworotko M, et al. Effects of crystal form on solubility and pharmacokinetics: a crystal engineering case study of lamotrigine. Cryst Growth Des. 2010;10(1):394–405.
10. Cheney ML, Weyna DR, Shan N, Hanna M, Wojtas L, Zaworotko MJ. Coformer selection in pharmaceutical cocrystal development: a case study of a meloxicam aspirin cocrystal that exhibits enhanced solubility and pharmacokinetics. J Pharm Sci. 2011;100(6):2172–81.
11. Báthori NB, Lemmerer A, Venter GA, Bourne AS, Caira MR. Pharmaceutical co-crystals with isonicotinamide–vitamin B3, clofibric acid, and diclofenac–and two isonicotinamide hydrates. Cryst Growth Des. 2011;11(1):75–87.
12. Sekhon BS. Drug-drug co-crystals. Daru. 2012;20(1):45.
13. Aitipumala S, Chow PS, Tan RBH. Trimorphs of a pharmaceutical cocrystal involving two active pharmaceutical ingredients: potential relevance to combination drugs. Cryst Eng Comm. 2009;11:1823–7.

14. Évora AOL, Castro ERA, Maria TMR, Rosado MTS, Silva MR, Beja AM, et al. Pyrazinamide–diflunisal: a new dual-drug co-crystal. Cryst Growth Des. 2011;11(11):4780–8.
15. Aitipumala S, Wong ABH, Chow PS, Tan RBH. Pharmaceutical cocrystals of ethenzamide: structural, solubility and dissolution studies. Cryst Eng Comm. 2012;14:8515–24.
16. Jiang l HY, Zhang Q, He H, Xu Y, Mei X. Preparation and solid-state characterization of dapsone drug-drug co-crystals. Cryst Growth Des. 2014;14(9):4562–73.
17. Sowa M, Slepokura K, Matczak-jon E. A 1:1 pharmaceutical cocrystal of myricetin in combination with uncommon piracetam conformer: X-ray single crystal analysis and mechanochemical synthesis. J Mol Struct. 2014;1058:114–21.
18. Daurio D, Medina C, Saw R, Nagapudi K, Alvarez-Núnez F. Application of twin screw extrusion in the manufacture of cocrystals, part I: four case studies. Pharmaceutics. 2011;3(3):582–600.
19. Fonseca JC, Clavijo JCT, Alvarez N, Ellena J. Novel solid solution of the antiretriviral drugs lamivudine and emtricitabine. Cryst Growth Des. 2018; https://doi.org/10.1021/acs.cgd.8b00164. ASAP
20. Lusi M. Engineering crystal properties through solid solutions. Cryst Growth Des. 2018; https://doi.org/10.1021/acs.cgd.7b01643. ASAP.
21. Trask AV. An overview of pharmaceutical cocrystals as intellectual property. Mol Pharm. 2007;4(3):301–9.
22. Tucker JL. Green chemistry, a pharmaceutical perspective. Org Process Res Dev. 2006;10(2):315–9.
23. Clark JH. Green chemistry: challenges and opportunities. Green Chem. 1999;1:1–8.
24. Constable DJC, Dunn PJ, Hayler JD, Humphrey GR, Leazer JL Jr, Linderman RJ, et al. Key green chemistry research areas—a perspective from pharmaceutical manufacturers. Green Chem. 2007;9:411–20.
25. Shan N, Jones WA. Green chemistry approach to the synthesis of a crystalline organic inclusion compound. Green Chem. 2003;5:728–30.
26. Weyna DR, Shattock T, Vishweshwar P, Zaworotko MJ. Synthesis and structural characterization of cocrystals and pharmaceutical cocrystals: mechanochemistry vs evaporation from solution. Cryst Growth Des. 2009;9(2):1106–23.
27. Friscic T, Jones W. Recent advances in understanding the mechanism of cocrystal formation via grinding. Cryst Growth Des. 2009;9(3):1621–37.
28. Hu Y, Gniado K, Erxleben A, McArdle P. Mechanochemical reaction of sulfathiazole with carboxylic acids: formation of a cocrystal, a salt, and coamorphous solids. Cryst Growth Des. 2014;14(2):803–13.
29. Bruni G, Maietta M, Berbenni V, Mustarelli P, Ferrara C, Freccero M, et al. Mechanochemical synthesis of bumetanide–4-aminobenzioc acid molecular cocrystals: a facile and green approach to drug optimization. J Phys Chem B. 2014;118(31):9180–90.
30. Karki S, Friscic T, Jones W, Motherwell WDS. Screening for pharmaceutical cocrystal hydrates via neat and liquid-assisted grinding. Mol Pharm. 2007;4(3):347–54.
31. Song J-X, Yan Y, Yao J, Chen J-M, Lu T-B. Improving solubility of lenalidomide via cocrystals. Cryst Growth Des. 2014;14(6):3069–77.
32. Jones W, Eddeleston MD. Introductory lecture: mechanochemistry, a versatile synthesis strategy for new materials. Faraday Discuss. 2014;170:9–34.
33. Haneef J, Chadha R. Drug-drug multicomponent solid forms: cocrystal, coamorphous and eutectic of three poorly soluble antihypertensive drugs using mechanochemical approach. AAPS PharmSciTech. 2017;18(6):2279–90.
34. Bowmaker GA. Solvent-assisted mechanochemistry. Chem Commun. 2013;49:334–48.
35. Malet-Martino M, Martino R. Clinical studies of three oral prodrugs of 5-fluorouracil (capecitabine, UFT, S–1): a review. Oncologist. 2002;7(4):288–323.
36. Vermes A, Guchelaar H-J, Dankert J. Flucytosine: a review of its pharmacology, clinical interactions, pharmacokinetics, toxicity and drug interactions. J Antimicrob Chemother. 2000;46(2):171–9.
37. Nishiyama T, Kawamura Y, Kawamoto K, Matsumura H, Yamamoto N, Ito T, et al. Antineoplastic effects in rets of 5-fluorocytosine in combination with cytosine deaminase capsules. Cancer Res. 1985;45(4):1753–61.
38. Zhang J, Kale V, Chen M. Gene-directed enzyme prodrug therapy. AAPS J. 2015;17(1):102–10.
39. Maleksha OM, Chen X, Nomani A, Sarkar S, Hatefi A. Enzyme/prodrug systems for cancer gene therapy. Curr Pharmacol Rep. 2016;2(6):299–308.
40. Christie C, Pomeroy A, Nair R, Berg K, Hirschberg H. Photodynamic therapy enhances the efficacy of gene-directed enzyme prodrug therapy. Photodiagn Photodyn Ther. 2017;18:140–8.
41. Funaro MG, Nemani KV, Chen Z, Bhujwalla ZM, Griswold KE, Gimi B. Effect of alginate microencapsulation on the catalytic efficiency and in vitro enzyme-prodrug therapeutic efficacy of cytosine deaminase and of recombinant E. coli expressing cytosine deaminase. J Microencapsul. 2016;33(1):64–70.
42. da Silva CCP, Pepino RO, de Melo CC, Tenorio JC, Ellena J. Controlled synthesis of new 5-fluorocytosine cocrystals based on the pKa rule. Cryst Growth Des. 2014;14(9):4383–93.
43. Rastogi VK, Palafox MA, Lang K, Singhal SK, Soni RK, Sharma R. Vibrtional spectra and thermodynamics of biomolecule: 5-chlorocytosine. Indian J Pure Appl Phys. 2006;44:653–60.